



UNIVERSITÀ
DEGLI STUDI
FIRENZE

FLORE

Repository istituzionale dell'Università degli Studi di Firenze

Polydopamine: surface coating, molecular imprinting, and electrochemistry—successful applications and future perspectives in

Questa è la Versione finale referata (Post print/Accepted manuscript) della seguente pubblicazione:

Original Citation:

Polydopamine: surface coating, molecular imprinting, and electrochemistry—successful applications and future perspectives in (bio)analysis / Palladino, Pasquale; Bettazzi, Francesca; Scarano, Simona*. - In: ANALYTICAL AND BIOANALYTICAL CHEMISTRY. - ISSN 1618-2642. - ELETTRONICO. - (2019), pp. 4327-4338. [10.1007/s00216-019-01665-w]

Availability:

This version is available at: 2158/1151597 since: 2022-09-14T14:05:40Z

Published version:

DOI: 10.1007/s00216-019-01665-w

Terms of use:

Open Access

La pubblicazione è resa disponibile sotto le norme e i termini della licenza di deposito, secondo quanto stabilito dalla Policy per l'accesso aperto dell'Università degli Studi di Firenze (<https://www.sba.unifi.it/upload/policy-oa-2016-1.pdf>)

Publisher copyright claim:

(Article begins on next page)



Polydopamine: successful applications and future perspectives in (bio)analysis and (bio)sensing

Journal:	<i>Analytical and Bioanalytical Chemistry</i>
Manuscript ID	Draft
Type of Paper:	Trends
Date Submitted by the Author:	n/a
Complete List of Authors:	Palladino, Pasquale; University of Florence, Chemistry 'Ugo Schiff' Bettazzi, francesca; Università di Firenze, Chemistry 'Ugo Schiff' Scarano, Simona; University of Florence, Chemistry 'Ugo Schiff'
Keywords:	Polydopamine, Molecularly Imprinted Polymers, Surface coating, Electrochemistry, Biosensing, Bioanalysis

SCHOLARONE™
Manuscripts



UNIVERSITÀ
DEGLI STUDI
FIRENZE

DIPARTIMENTO
DI CHIMICA
"UGO SCHIFF"

December, 7th 2018

Dear Dr Maria Teresa Menes Vazquez,

we are sending the manuscript entitled: "Polydopamine: successful applications and future perspectives in (bio)analysis and (bio)sensing" by P. Palladino, F. Bettazzi, and S. Scarano*, which we would like you consider for publication as *Trend Article* as ABC young investigators special issue (invited contribution).

We believe that our manuscript is of interest for the *ABC* readership because it proposes a short survey on polydopamine applications for surface coating, molecular imprinting, and electrochemistry. Nonetheless, the peculiar physicochemical properties of dopamine and its polymer, due to the reduction potential of catechol moiety, are not fully exploited. We have confidence in possibility to spread its applications through a large variety of research approaches, including the use of naturally occurring or synthetic dopamine analogues and co-polymers. Accordingly, our efforts in this direction are focused in proposing the role of this polymer for quantitative applications, evaluating analytical performances, costs, reproducibility and versatility of the developed methods also revisiting standard (bio)analytical platforms.

Our manuscript has been written according to the *Instructions for Authors*, but we are ready to modify anything you will suggest. Furthermore, hereby we confirm that it has not been published previously by any of the authors and is not under consideration for publication in another journal.

Thank you for your consideration.

Simona Scarano, PhD

Corresponding Author:

E-mail: simona.scarano@unifi.it

Department of Chemistry 'Ugo Schiff', University of Florence

50019 Sesto Fiorentino (FI), Italy.

Phone: +390554573283

Suggested referees:

1) Prof. Eric Peyrin (eric.peyrin@univ-grenoble-alpes.fr)

Université Grenoble Alpes, Département de Pharmacochimie Moléculaire – UMR 5063, France.

2) Prof. Giuseppe Spoto (spotog@unict.it)

Università di Catania, Dipartimento di Scienze Chimiche, Italy.

3) Dr. Jakub Dostalek, PhD (jakub.dostalek@ait.ac.at)

AIT Austrian Institute of Technology GmbH, 1190 Wien, Austria.

Polydopamine: successful applications and future perspectives in (bio)analysis and (bio)sensing

P. Palladino, F. Bettazzi, S. Scarano*

*Corresponding author: simona.scarano@unifi.it

Department of Chemistry 'Ugo Schiff', University of Florence, via della Lastruccia 3-13, 50019, Sesto Fiorentino, Firenze

Abstract

Dopamine oxidation and self-polymerization has recently gained a large interest arising from the versatile chemistry of this endogenous catecholamine. Particularly stimulating appear the applications of this biopolymer for surface coating, molecular imprinting, and electrochemistry, here reviewed, covering the broad fields of medicine, material science, and (bio)analytical chemistry. Nonetheless, the peculiar physicochemical properties of dopamine and its polymer, due to the reduction potential of catechol moiety, are not fully exploited. We have confidence in possibility to spread its applications through a large variety of research approaches, including the use of naturally occurring or synthetic dopamine analogues and co-polymers. Accordingly, our efforts in this direction are focused in proposing the role of this polymer for quantitative applications, evaluating analytical performances, costs, reproducibility and versatility of the developed methods also revisiting standard (bio)analytical platforms.

Keywords Polydopamine, Molecularly Imprinted Polymers, Surface coating, Electrochemistry, Biosensing, Bioanalysis

1. Introduction

The huge significance of endogenous Dopamine (DA) for human renal, hormonal and central nervous systems, and the consequent severe clinical conditions associated with DA concentration anomalies, including Schizophrenia, and Parkinson's disease, has generated more than 200 thousand scientific papers over the past 80 years. A more recent and intriguing outcome from this plethora of information is represented by DA oxidation and self-polymerization [1-3]. The electrochemical and chemical

1
2
3 reaction pathway for polydopamine (PDA) formation in aqueous solutions requires the synthesis of
4 5,6-indolequinone (IQ) monomer from dopamine molecule [1,4,5]. Notably, the polymer growth is
5 inhibited by low pH (below 4) and high-concentration of various electrolytes that impair the
6 preliminary intramolecular cyclization of oxidized dopamine by decreasing the nitrogen
7 nucleophilicity [1]. Since the pioneering investigations and application on dopamine polymerization
8 by electrodeposition [1,2], and then by O₂/pH-induced oxidation [3], thousands of papers involving
9 the PDA synthesis, study and application have been published. Notably, the last four years represent
10 almost 80% of all the scientific production, underlining the enhanced interest arising from the
11 versatile chemistry of this endogenous catecholamine and its complex polymerization mechanism [6-
12 9]. The reactivity of dopamine and its polymer is associated to the reduction potential of catechol
13 moiety that has been exploited to produce optically and catalytically active metal nanoparticles *in situ*
14 [10-12]. This feature responsible for the cross-linking of dopamine can be enhanced by chemical
15 oxidants [13-15], UV [16], or microwave irradiation [17], influencing the coating of PDA at
16 nanometric scale employed for a variety of physical, chemical and biological studies [7, 8]. However,
17 this field of research is still young and challenging in application of PDA-coated surface to medicine,
18 energy and industrial manufacturing, for example [7,8]. In particular, a promising field of PDA
19 research is the surface coating for molecular sensing and affinity separation for pharmaceutical
20 studies and clinical applications [18,19], following the peculiar physicochemical properties of PDA,
21 including the photo/thermo/electro/chemical reactivity [10-12], and the molecular immobilization
22 and imprinting capability of this biopolymer [2, 20-23]. Here we report a survey of this demanding
23 area of bioanalytical research, focusing on the state-of-art of PDA applications for coating,
24 imprinting, and electrochemistry, and offering a long-term vision for the capability of this polymer
25 to be exploited to its full potential.
26
27
28
29
30
31
32
33
34
35
36
37
38
39
40
41
42
43
44
45

46 **2. Polydopamine imprinting**

47
48 The preparation of molecularly imprinted polymers (MIPs) requires non-covalent interactions or
49 formation of reversible covalent adducts between a molecular template of interest and functional
50 monomer(s) prior to the polymerization of the latter. Subsequent template removal generates
51 synthetic binding sites within the polymer with high selectivity and sensitivity toward the template
52 molecule [24-27]. In this framework, dopamine appears particularly suitable for molecular imprinting
53 thanks to its hydrophilicity, biocompatibility, self-assembling, and universal coating capability [3,7].
54 In particular, the simple dopamine-analyte co-polymerization and the subsequent analyte removal has
55 been used to generate a robust and biocompatible nanometric film for quantitative analysis of
56
57
58
59
60

1
2
3 molecule without an additional self-assembled sublayer. Here we review selected publications useful
4 to categorize the research lines for PDA application in MIP based on substrate geometry and
5 composition, or following the template size (Fig. 1).
6
7

8 9 *2.1 MIP substrates: geometry and composition*

10
11 Among the variety of PDA layer applications [18,19,21], PDA adhesion for molecular
12 imprinting is essentially associated to solid phase extraction and microextraction [18]. The majority
13 of these functional nanocomposites are nanoparticles (NPs), and materials with similar geometry like
14 carbon dots (CDs) and quantum dots (QDs). Less abundant are the studies involving the PDA coating
15 and imprinting on nanotubes (NTs), graphite oxide (GO), macroscopic surfaces (gold and quartz),
16 and hydrogels [18]. Commonly, the deposition and imprinting has been studied via scanning electron
17 microscopy (SEM), transmission electron microscopy (TEM), dynamic light scattering (DLS), and
18 atomic force microscopy (AFM) before and after the polymer adhesion to determine the
19 morphological features, *i.e.* shape, size distribution and dispersibility of nanocomposites and
20 topography of extended surfaces.
21
22

23
24 *2.1.1 MIP on Nanoparticles.* The size of the imprinted particles is dependent on the synthetic protocol
25 and may differ of some orders of magnitudes, determining huge differences between the preparations
26 in terms of amount of PDA per nanoparticle, and, more in general, the surface-to-volume ratio and
27 the properties of the nanocomposites. In detail, magnetic molecularly imprinted polymers (MMIP)
28 are built using a core of Fe_3O_4 , which can contain additional shells, mainly SiO_2 , contributing to the
29 global structural and physical features of MMIPs [18]. However, the outer shell of PDA constituting
30 the MIP is independent from substrate size and composition, appearing tunable in a thickness range
31 of 5-100 nm for a single growth step [28-31]. For example, very small fluorescent carbon dots with
32 magnetic Fe_3O_4 core (mean diameter around 12 nm) have been coated with a shell of PDA of about
33 25 nm [32]. Nevertheless, much larger particles (up to micrometer) still preserve an outer shell of
34 PDA with similar size [33,34,35].
35
36
37
38
39
40
41
42
43
44
45
46
47

48
49 *2.1.2 MIP on Nanotubes.* Porous tubular structure at nanometric scale has been reported in form of
50 carbon nanotubes (CNTs), multi-walled carbon nanotubes (MWNTs), halloysite nanotubes (HNTs),
51 [36-40] and their magnetic counterparts are obtained by Fe_3O_4 nanoparticles grafted onto nanotubes
52 [36,39]. The outer diameter of nanotubes is variable, but in the range of a few tens of nanometers [36-
53 40]. The PDA-coating shell before and after the template imprinting procedures ranges between very
54 few nanometers [36-38, 40] to a thickness of 40 nm [39]. Although morphology changes for imprinted
55 nanotubes upon analyte rebinding have not been reported, notably, a smaller thickness of MIP in
56 comparison with NIP has been ascribed to dopamine polymerization inhibition by template [38]. Very
57
58
59
60

peculiar appear the HNTs owning a chemically reactive hollow tubular structure, which can assume negatively charged silica layer on the outer surface and positively charged alumina layer on the inner surface. Although successfully imprinted, the coating layer appears not uniform likely because of redox properties of HNTs surface [40].

2.1.3 *MIP on Flat surfaces*. Bidimensional imprinting (2D-MIP) has been achieved by PDA adhesion on molecular (GO) or extended (Au/SiO₂) flat surfaces. In detail, sheets of GO have been commonly synthesized from graphite and then coated with PDA, thus obtaining a larger surface-to-volume ratio, and a higher number of binding sites per volume, in comparison to nanoparticles [41]. Nevertheless, Fe₃O₄ NPs can be also deposited on GO sheets prior of imprinting to confer magnetic properties to these substrates [41]. Electron microscopy images show curved surface for these nanocomposites before and after the imprinting [41,42]. Furthermore, the 2D-MIP morphology analysis (AFM, SEM) allows to observe both the thickness of GOs (ca. 1 nm) and the PDA adhesion layer (few nanometers) [42]. There are not observable differences between MIP and NIP because the size of template and, consequently, the dimensions of its binding site are below the limit of resolution of the microscopy techniques. On the other hand, this morphology conservancy of nanocomposites upon imprinting, template removal, and its rebinding, confirms the stability of the PDA layer and gives an indirect proof that the larger binding capacity of MIP in comparison to NIP has to be ascribed to the effective molecular imprinting and not to PDA not-specific assembly modification. Regarding the extended deposition and imprinting of PDA, gold chips or SiO₂ bare crystals has been employed as substrates for molecular detection and analysis via surface plasmon resonance (SPR), quartz crystal microbalance (QCM), and electrochemical (EC) techniques [20,43-45]. Based on theoretical design, the PDA thickness has been tuned between few and few tens of nanometers to obtain the best template orientation during the molecular imprinting. This to achieve the most analyte-accessible functional cavities into polymer layer [43]. Surface morphology of bare substrate, NIP and MIP have been usually investigated by AFM [44,45] measuring film thickness, roughness, and homogeneity after coating, imprinting and washing stages, leading to a topographic characterization of PDA deposition and imprinting [45].

2.2 *MIP templates size: Mesoscopically Imprinted Polymers*

The first example reported in the literature involved a PDA-based molecularly imprinted polymer (MIP) for the capacitive sensing of nicotine [2]. Later on, PDA has been employed as recognition element of much larger targets, like proteins, or viruses. Therefore, it appears reasonable that several new applications of PDA-based MIP will be related to the imprinting and sensing of living cells and viruses in biological and environmental samples. This expansion of MIP applicability as specific

1
2
3 recognition element of larger and much more complex analytes has been possible thanks to self-
4 assembling of dopamine in aqueous media that generates a biocompatible polymer. In fact, PDA-
5 unique features have easily overwhelmed the problem associated to poor stability of biological
6 molecules in organic solvents previously necessary for solubilization and reaction of other kind of
7 functional monomers and cross-linking agents. Consequently, mesoscopically imprinted polymers
8 appears a more suitable and comprehensive name for the current and future developments of
9 biopolymers imprinting strategy in biosensing.

16 *2.2.1 Small molecules imprinting*

17
18 To the best of our knowledge, nicotine has been the first molecule imprinted in PDA for molecular
19 detection [2], anticipating plentiful applications in MIPs sensors development, mostly by using
20 nanoparticles as substrate. In particular, the imprinting of small molecules ($0.1 \text{ kDa} < \text{MW} < 1 \text{ kDa}$)
21 has regarded amino acids [33], estrogens [34], flavorings [37], colorants [38], phenolic acids [39],
22 toxins [44], antibiotics [45], sugars [46], and chemotherapeutic agents in cancer [47]. Notably, it has
23 been reported that the release of an anticancer molecule imprinted on PDA-coated Fe_3O_4
24 nanoparticles increases in presence of a magnetic field, resulting in an effective control of tumor
25 growth in animal models [47], thus paving the way for future studies and applications of MIPs on
26 magnetic substrates.

34 *2.2.2 Oligonucleotides, enzymes, and immunoglobulins imprinting*

35
36 After an early report on human hemoglobin-imprinted PDA showing high rebinding capacity and
37 specific recognition in aqueous media [48], several PDA-imprinted substrates have been developed
38 for rapid and specific recognition of proteins and oligonucleotides with potential application to
39 separation of analytes from real and complex matrices [21]. The adsorption selectivity and binding
40 specificity has been evaluated comparing MIPs and NIPs towards the template calculating the
41 imprinting factor (IF), and towards competitive analytes with similar shape, size and isoelectric
42 points, i.e. the selectivity coefficient (SC). For example, studies on BSA imprinting and separation
43 from blood samples have given values of IF between 1.7 and 6.2 and SC between 1.3 and 4.5
44 [40,41,49]. Similar studies have been reported for different oligonucleotides, enzymes,
45 immunoglobulins with a molecular weight ranging from 7 to 150 kDa, up to a few tens of nanometers
46 in length [21].

56 *2.2.3 Viruses imprinting*

57
58 Very recently, trace amounts of several viruses have been directly and specifically detected by using
59 virus-imprinted PDA. Namely, Hepatitis A Virus (HAV) and bacteriophages (f2, T4, P1, and M13)

[23, 50,51]. In case of HAV, sensing has been achieved also in human serum by using virus-imprinted SiO₂@PDA, or magnetic Fe₃O₄@PDA, NPs with a low limit of detection down to ca. 10⁻¹¹ M and an imprinting factor (IF), i.e. the binding capacity ratio between MIP and NIP, around 2 [50,51]. Remarkably, electron microscopy images of modified nanoparticles present surface protuberances between the PDA-imprinting and washing stages, and hollows after template removal, with a size and shape compatible with the HAV units (30 nm in diameter), giving a direct evidence of the virus imprinting. In case of bacteriophages reported above, it has been shown that the virus morphology severely affects the PDA imprinting on silica particles, and consequently its binding selectivity and kinetics, that get worse with size increase from the smallest and spherical phage f2 (ca. 26 nm in diameter) to the largest and elongated phage M13 (900 nm) [23]. However, the authors recognize that the apparent negative correlation between dimensions and imprinting requires further investigations to exclude other factors, e.g. the influence of specific capsid proteins of the investigated viruses [23].

3. Electrochemical and photoelectrochemical characterization and exploitation of PDA films in sensing and biosensing

Due to their intrinsic characteristics of being potentially fast, easy and low cost, electrochemical and photoelectrochemical techniques are widely used for the development of bioassays for the detection of analytes of clinical interest such as clinical biomarkers [52,53]. Therefore, sensor surface modification strategies are often challenging because biosensing applications require highly biocompatible and properly functionalized surfaces to bind the biorecognition material and retaining its biological activity. Moreover, the binding should be sufficiently strong to avoid the leaching of the biomaterial from the sensors surface [54]. The increasing need of easy, efficient and versatile immobilization methods in bioanalytical assays development lead to the investigation of the PDA potential applications.

3.1 Deposition of a polydopamine layer on an electrode: chemical oxidation vs electrodeposition

The fundamental mechanism of the formation of PDA is still not fully understood [55,56]. In most of the applications, the polymerization of dopamine is achieved via the chemical process reported by Lee et al. [3]. Briefly, a combination of bulk and surface polymerization is induced at a basic pH. Simple immersion of substrates in a dilute aqueous solution of dopamine, buffered at typical marine environments pH (10 mM tris, pH 8.5), resulted in spontaneous deposition of a thin adherent polymeric film. Polymerization occurs involving the oxidation of catechol to quinone that further

1
2
3 reacts with amine and the other catechols and quinones, leading to the formation of the polymeric
4 film. Despite the film is not chemically homogeneous, the coating obtained with this straightforward
5 procedure shows a great reactivity toward amine and thiol groups [54,57-58]. Such kind of coatings,
6 often called pseudo-melanin, can be also easily modified as single step reaction leading to several
7 kinds of modified surfaces including metal nanoparticle decorated surface [59-61], such as silver NPs
8 [62] or gold NPs [63,64], via the reduction from solution of the corresponding cations. This reduction
9 step is possible through the presence of the catechol groups that undergo an oxidation at the quinone
10 functional groups during the reduction of the metallic cations. This reactivity of residual quinone
11 groups in PDA films could be advantageously exploited for the covalent immobilization of
12 biomolecules [65,66] for biosensor development [54,67].

13
14
15
16
17
18
19
20
21 A possible drawback of this method is the difficulty in controlling the localization and the surface
22 morphology of the deposited PDA film. Despite this polymerization strategy is easily reproducible
23 and universally established for a wide range of materials [65], an alternative method for the
24 preparation of PDA can be achieved by an electrochemical polymerization process. Since the electro-
25 polymerization occurs just at the interface of the electrode, PDA films can be generated in a highly
26 controlled and spatially selective manner. The mechanism of PDA electro-polymerization has been
27 thus deeply investigated since the late seventies [68, 69], in which Adams et al. proposed essentially
28 two electrochemical mechanisms related to DA oxidation namely the so-called ECC and ECE
29 mechanisms (where E and C denotes the electrochemical and the chemical step, respectively). The
30 oxidation of DA is considered to finally leading to melanin-like polymers and thus the result of the
31 whole process is complex. In the ECE mechanism the polymerization goes through three steps: in the
32 first step the formation of o-dopaminoquinone occurs after exchange of two electrons and two
33 protons. It is commonly known that the quinones are quite reactive and can undergo nucleophilic
34 coupling. Depending on the experimental conditions used, mechanisms with more complicated
35 sequences electrochemical and chemical steps were also proposed [65, 69]. Dopaminoquinone
36 contains both an electron-deficient ring and an electron-donor amine group. As the results of a 1,4
37 Michael addition and upon deprotonation of the amine group, a cyclization reaction can occur.
38 Therefore, in the second step the o-dopaminoquinone undergoes intramolecular cyclization which
39 leads to leucodopaminochrome, which is easily oxidized in the third step to dopaminochrome that
40 may be transformed into melanin polymers.

41
42
43
44
45
46
47
48
49
50
51
52
53
54
55
56
57
58
59
60
60 Voltammetric studies of DA have further elucidated the oxidation steps leading to PDA formation
[70, 71], In detail, during the consecutive scans, has been reported a continuous decrease of the peak
current intensities, due to the formation of PDA layers (Fig. 2a-b). This effect demonstrates that the
electrode surface is affected by the fouling of the electrode caused by the PDA layers as it grows with

1
2
3 successive scans up to a complete electrode fouling. Nevertheless, two redox peaks are still present
4 and can be attributed to the oxidation and reduction of the catechols and quinones units present in
5 PDA [55,72]. Furthermore, the linearity of the anodic and cathodic peak currents versus scan rate
6 indicates a surface confined voltammetry corresponding to a “thin layer” type [71], and the electrode
7 transfer reaction appears controlled by both adsorption and diffusion [70]. The effect of the pH
8 showed that the oxidation peak potential moves to lower values with increasing the solution pH,
9 indicating the involvement of protons in the electrochemical reaction [71]. These features have been
10 also exploited in the fabrication of a pH sensor based on glassy carbon electrodes and PDA films
11 [55].

12
13 It clearly appears that the accurate assignment of all the redox processes occurring on PDA films is a
14 challenging task [54]. The easy and universal application of PDA and the wide variety of exploitation
15 in sensing and biosensing assays development is in contrast with the complex electrochemical
16 behavior. Moreover, this is also in contrast to the well-established redox processes of common
17 conducting polymers, such as polypyrrole, polythiophene, or polyaniline [73,74].

18 19 20 21 22 23 24 25 26 27 28 29 30 31 32 33 34 35 36 37 38 39 40 41 42 43 44 45 46 47 48 49 50 51 52 53 54 55 56 57 58 59 60

3.2 Photo-electrochemical properties of PDA and photoelectrochemical bioassays

Photoelectrochemical (PEC) biosensors are powerful and reliable tools for bioanalysis, due to the
inherent operational simplicity, low back-ground current and high detection sensitivity [75-77].
Recently, photoelectrochemistry has been applied to the detection of several analytes, such as H₂O₂
[78], microRNA [77], nucleic acids [79], proteins [80] and glucose [81].

The effectiveness of the PEC assay mainly relies on the performance of the photo-active material.
Recent studies demonstrated that quinones can be successfully exploited in energy applications
through the hybridization of these of molecules with several kind of materials [82, 83]. In this
framework, some recent reports demonstrated that the synthesized PDA exhibited semiconducting
properties and special charge transfer capability inferred by the presence of the π - π system. The
presence of a highest occupied molecular orbital (HOMO) and a lowest unoccupied molecular orbital
(LUMO) makes PDA a useful photosensitizer, to promote the absorption of visible light, improving
light harvesting efficiency and charge collection efficiency in PEC bioassays (Fig. 2c) and offering
interesting opportunities for high-performance optoelectronic devices development [83,84].

4. Future outlooks on the role of polydopamine in bioanalytical chemistry

1
2
3 The intriguing versatility of PDA has drawn its relevant role in a number of research fields,
4 first of all in the science of biocompatible materials for drug delivery and cancer therapy.
5 Undoubtedly, the auto-assembling and coating abilities of this polymer are the most exploited features
6 in such applications. Functional surface moieties (quinones/cathecols and amines) add further
7 facilities in the subsequent (bio)chemical modification of PDA coatings, expanding their role beyond
8 expectations. However, at present it is surprising the lack of innovative uses of PDA in the field of
9 (bio)analytical chemistry, excluding those aforementioned for the synthesis of MIPs and, in general,
10 for electrochemical-based applications. In this framework, original and unexplored ways of looking
11 for the possible use of dopamine/polydopamine with direct impact in quantitative (bio)analytics are
12 under study. One of the poorly investigated aspects of DA polymerization to give PDA films is the
13 kinetics of formation of these layers at the surface of the considered material. For example, during
14 the formation of the PDA adhesive layer at polystyrene surface (*i.e.* disposable laboratory equipment
15 such as microtiter plates, UV-Vis cuvettes, tips etc.), the polymerization step may be perturbed in
16 significant ways to obtain analytical information useful for macromolecules, *i.e.* protein detection in
17 complex matrices [9].
18
19
20
21
22
23
24
25
26
27
28

29 In particular, the co-presence in solution of proteins directly impairs the thickness of the final PDA
30 layer adhered on the substrate [9]. This approach, considered until now a drawback in MIP production
31 for protein detection, deserves on the contrary further investigations. The broad absorption band of
32 PDA in the visible range permits to investigate the optical response at almost any wavelength, and on
33 low-cost and widely used plate readers commonly used in immune-based assays (*i.e.* ELISA). The
34 perspective application of such a bioanalytical method would open new and crucial scenarios in favor
35 of the serious fails of current methods for quantification of total protein in biological fluids (Fig. 3a).
36 Behind this, application to nanoplasmonic-based detection of low molecular weight analytes has been
37 very recently reported. In particular, our group has explored the possibility of developing 'Plasmonic
38 cuvettes' by *in-situ* growth of controlled AuNPs by PDA, for Localized Surface Plasmon Resonance
39 (LSPR)-based quantitative assays at fixed wavelength, using a conventional spectrophotometer [11].
40 This research starts from the consideration of the role of PDA films decorated with metal
41 nanoparticles. Despite the presence of numerous papers dealing with the *in-situ* reduction of metal
42 ions at PDA surface to obtain nanoparticles, no indication on the rationale behind the process is
43 provided; we recently obtained some results in that direction, both by modulating the PDA formation
44 protocol [11] before its exposure to Au(III), and by varying the metal ion concentration leaving fixed
45 the PDA film features [12]. In the first case, we clarify the crucial role played by PDA morphology
46 in obtaining different populations of gold NPs, providing different plasmonics behaviors. The
47 surprising evidence is that not only the reducing power of PDA towards Au(III) increases linearly
48
49
50
51
52
53
54
55
56
57
58
59
60

with thickness, but also that the plasmonic behavior of AuNPs changes accordingly. Considering the increasing demand of low-cost protocols to modulate different LSPR regimes for biosensing applications [85, 86], this result stimulated further investigation. In fact, deposited nanostructures with different features (size, geometry, density, etc.) generally express a hybrid behavior between pure wavelength sensitivity (S_{λ} , nm RIU⁻¹) at constant extinction, and pure absorbance sensitivity (S_{Abs} , Abs RIU⁻¹) at constant wavelength. The significant result is that PDA thickness is able to modulate the plasmonic response from the classical wavelength shift to the absorbance intensity one (Fig. 2b). This approach was applied to the quantitative determination of fermentable sugars in beer wort, with excellent analytical performances compared to routine refractometers used in cellars. Moreover, the easy reading of the 'photonic' UV-Vis cuvettes at fixed wavelength on portable spectrometers allows to figure out further applications in clinical, food, and environmental controls. PDA-based nanocomposites for quantitative assays based on catalytic activity of metal NPs may represent a further easy and low-cost approach for colorimetric determination of (bio)analytical targets in human specimens [12]. In other words, by going deeper in understanding of PDA behavior, novel analytical applications can be developed by combining PDA redox characteristics and kinetic of film formation.

By the reverse approach, once fixed the PDA film typology, the role of different metal ion concentrations in producing different AuNPs populations deserves also further investigation. In this context, PDA films decorated with *in-situ* grown AuNPs (AuNPs@PDA) substrates were tested for their catalytic activity towards nitrophenol (NPh) isomers. As widely reported in literature, AuNPs (in solution or supported) act as efficient catalysts in a large variety of organic reduction and oxidation reactions. But, to now, the reduction of NPhs and in particular of p-NPh has been reported prevalently as case study to characterize and compare different catalytic substrates, whereas for its quantitative determination HPLC and HPLC-MS with the use of radiolabels generally remain the techniques of choice. In a recent study, the *in-plate*, fast, low-cost, and high throughput determination of p-NPh on AuNPs@PDA substrates in aqueous solution and in urine was achieved, providing very new information on the behavior of these nanocomposites during the catalytic process. Different AuNPs populations may show different catalytic ability and chemical resistance on the base of the preparation protocol (in terms of Au(III) concentration) used. Only a specific concentration range of Au(III) guarantees AuNPs@PDA resistant to the reduction process, whereas out of this range the complete dissolution of the nanocomposite occurs. The result is easily obtained by a routine ELISA reader at 415 nm, where the absorbance decreases of the p-nitrophenolate ion (the optically active species generated by p-NPh with an excess of NaBH₄) gives quantitative and linearly correlated information on the p-NPh present in the sample (Fig. 3c). Concluding, recent advancements on PDA decorated

1
2
3 with metallic nanoparticles widen the possibilities in this emerging field. Several metallic precursors
4 are reducible at PDA surface, giving NPs with different and exciting optical, catalytic, and functional
5 properties. Therefore, we envisage that the development of innovative PDA-based nanocomposites
6 applicable to bioanalytical chemistry will mark the near future also in the (bio)analytic chemistry.
7
8
9

10 As a whole, PDA consists in a very promising tool not only in the already explored fields of applied
11 medicine and in material science, but also in the near future of (bio)analytical chemistry. Our efforts
12 in this direction are focused in proposing the role of this polymer for quantitative applications,
13 evaluating analytical performances, costs, reproducibility and versatility of the developed methods
14 also revisiting standard platforms, as ELISA readers, portable spectrophotometers and
15 electrochemical devices. The reactivity of DA to give PDA in different environmental conditions
16 remains only partially explored, and we have concrete indications in several directions to push up its
17 use through a large variety of strategies, also involving dopamine homologues and other suitable co-
18 polymers playing different roles in this extremely fast raising research field.
19
20
21
22
23
24
25
26
27
28

29 **Acknowledgments**

30 Authors thank the Ministry of Education, University and Research (MIUR) for financial support
31 through the scientific program SIR2014 Scientific Independence of young Researchers
32 (RBSI1455LK), Horizon 2020, European Union Funding for Research & Innovation, and Regione
33 Toscana for the scientific program PLABAN PLAsmonic Biosensors ANalysis of nucleic acid
34 biomarkers (D53D16002290009).
35
36
37
38
39
40
41
42
43
44
45
46
47
48

49 **Conflict of interest**

50 The authors declare that they have no conflict of interest.
51
52
53
54
55

56 **References**

- 57
58 1. Li Y, Liu M, Xiang C, Xie Q, Yao S. Electrochemical quartz crystal microbalance study on
59 growth and property of the polymer deposit at gold electrodes during oxidation of dopamine
60

- 1
2
3 in aqueous solutions. *Thin Solid Films*. 2006; 497(1-2): 270-278.
4 <https://doi.org/10.1016/j.tsf.2005.10.048>.
- 5
6
7 2. Liu K, Wei WZ, Zeng JX, Liu XY, Gao YP. Application of a novel electrosynthesized
8 polydopamine-imprinted film to the capacitive sensing of nicotine. *Anal Bioanal Chem*. 2006;
9 385(4): 724-729. <https://doi.org/10.1007/s00216-006-0489-z>.
- 10
11
12 3. Lee H, Dellatore SM, Miller WM, Messersmith PB. Mussel-inspired surface chemistry for
13 multifunctional coatings. *Science*. 2007; 318(5849): 426-430.
14 <https://doi.org/10.1126/science.1147241>.
- 15
16
17 4. Hawley MD, Tatawawadi SV, Piekarski S, Adams RN. Electrochemical studies of the
18 oxidation pathways of catecholamines. *J Am Chem Soc*. 1967; 89(2): 447-450.
19 <https://doi.org/10.1021/ja00978a051>.
- 20
21
22 5. Saraji M, Bagheri A. Electropolymerization of indole and study of electrochemical behavior
23 of the polymer in aqueous solutions. *Synth Met*. 1998; 98(1): 57-63.
24 [https://doi.org/10.1016/S0379-6779\(98\)00151-9](https://doi.org/10.1016/S0379-6779(98)00151-9).
- 25
26
27 6. Yang J, Stuart MAC, Kamperman M. Jack of all trades: versatile catechol crosslinking
28 mechanisms. *Chem Soc Rev*. 2014; 43(24): 8271-8298. <https://doi.org/10.1039/c4cs00185k>.
- 29
30
31 7. Ryu JH, Messersmith PB, Lee H. Polydopamine surface chemistry: a decade of discovery.
32 *ACS appl mater interfaces*. 2018; 10(9), 7523-7540. <https://doi.org/10.1021/acsami.7b19865>.
- 33
34
35 8. Qiu WZ, Yang HC, Xu ZK. Dopamine-assisted co-deposition: An emerging and promising
36 strategy for surface modification. *Adv Colloid Interface Sci*. 2018; 256:111-125.
37 <https://doi.org/10.1016/j.cis.2018.04.011>.
- 38
39
40 9. Palladino P, Britto A, Pascale E, Minunni M, Scarano S. *Talanta*. 2018; under review.
- 41
42
43 10. Wang JG, Hua X, Li M, Long YT. Mussel-Inspired Polydopamine Functionalized Plasmonic
44 Nanocomposites for Single-Particle Catalysis. *ACS Appl Mater Interfaces*. 2017; 9(3):3016-
45 3023. <https://doi.org/10.1021/acsami.6b14689>.
- 46
47
48 11. Scarano S, Pascale E, Palladino P, Fratini E, Minunni M. Determination of fermentable sugars
49 in beer wort by gold nanoparticles@ polydopamine: A layer-by-layer approach for Localized
50 Surface Plasmon Resonance measurements at fixed wavelength. *Talanta*. 2018; 183:24-32.
51 <https://doi.org/10.1016/j.talanta.2018.02.044>.
- 52
53
54 12. Scarano S, Palladino P, Pascale E, Britto A, Minunni M. *Microchim Acta*. 2018; under
55 review.
- 56
57
58 13. Wei Q, Zhang F, Li J, Li B, Zhao C. Oxidant-Induced Dopamine Polymerization for
59 Multifunctional Coatings. *Polym Chem*. 2010; 1:1430-1433.
60 <https://doi.org/10.1039/c0py00215a>.

14. Hong SH, Hong S, Ryou MH, Choi JW, Kang SM, Lee H. Sprayable Ultrafast Polydopamine Surface Modifications. *Adv Mater Interfaces*. 2016; 3:1500857. <https://doi.org/10.1002/admi.201500857>.
15. Ponzio F, Barthès J, Bour J, Michel M, Bertani P, Hemmerlé J, d'Ischia M, Ball V. Oxidant Control of Polydopamine Surface Chemistry in Acids: A Mechanism-Based Entry to Superhydrophilic-Superoleophobic Coatings. *Chem Mater*. 2016; 28: 4697–4705. <https://doi.org/10.1021/acs.chemmater.6b01587>.
16. Du X, Li L, Li J, Yang C, Frenkel N, Welle A, Heissler S, Nefedov A, Grunze M, Levkin PA. UV-Triggered Dopamine Polymerization: Control of Polymerization, Surface Coating, and Photopatterning. *Adv Mater*. 2014; 26:8029-8033. <https://doi.org/10.1002/adma.201403709>.
17. Lee M, Lee SH, Oh IK, Lee H. Microwave-Accelerated Rapid, Chemical Oxidant-Free, Material-Independent Surface Chemistry of Poly(dopamine). *Small*. 2017; 13:1600443. <https://doi.org/10.1002/smll.201600443>.
18. Li H, Jia Y, Peng H, Li J. Recent developments in dopamine-based materials for cancer diagnosis and therapy. *Adv Colloid Interface Sci*. 2018; 252:1-20. <https://doi.org/10.1016/j.cis.2018.01.001>.
19. Barclay TG, Hegab HM, Clarke SR, Ginic-Markovic M. Versatile surface modification using polydopamine and related polycatecholamines: Chemistry, structure, and applications. *Adv Mater Interfaces*. 2017; 4(19):1601192. <https://doi.org/10.1002/admi.201601192>.
20. Palladino P, Minunni M, Scarano S. Cardiac Troponin T capture and detection in real-time via epitope-imprinted polymer and optical biosensing. *Biosens Bioelectron*. 2018; 106:93-98. <https://doi.org/10.1016/j.bios.2018.01.068>.
21. Che D, Cheng J, Ji Z, Zhang S, Li G, Sun Z, You J. Recent advances and applications of polydopamine-derived adsorbents for sample pretreatment. *Trends Anal Chem*. 2017; 97:1-14. <https://doi.org/10.1016/j.trac.2017.08.002>.
22. Chen D, Mei Y, Hu W, Li CM. Electrochemically enhanced antibody immobilization on polydopamine thin film for sensitive surface plasmon resonance immunoassay. *Talanta*. 2018; 182:470-475. <https://doi.org/10.1016/j.talanta.2018.02.038>.
23. Li N, Liu YJ, Liu F, Luo MF, Wan YC, Huang Z, Liao Q, Mei FS, Wang ZC, Ji AY, Shi Y, Lu B. Bio-inspired virus imprinted polymer for prevention of viral infections. *Acta Biomater*. 2017; 51:175-183. <https://doi.org/10.1016/j.actbio.2017.01.017>.
24. Wulff G. Molecular Recognition in Polymers Prepared by Imprinting with Templates. *ACS Symposium Series*. 1986; Vol. 308, Chapter 9, pp 186–230. <https://doi.org/10.1021/bk-1986-0308.ch009>.

- 1
2
3 25. Zamora-Galvez A, Morales-Narváez E, Mayorga-Martinez CC, Merkoçi A. Nanomaterials
4 connected to antibodies and molecularly imprinted polymers as bio/receptors for bio/sensor
5 applications. *Appl Mater Today*. 2017; 9:387-401.
6
7 <https://doi.org/10.1016/j.apmt.2017.09.006>.
8
9
10 26. Dabrowski M, Lach P, Cieplak M, Kutner W. Nanostructured molecularly imprinted
11 polymers for protein chemosensing. *Biosens Bioelectron*. 2017; 102, 17-26.
12
13 <https://doi.org/10.1016/j.bios.2017.10.045>.
14
15 27. Gui R, Jin H, Guo H, Wang Z. Recent advances and future prospects in molecularly
16 imprinted polymers-based electrochemical biosensors. *Biosens Bioelectron*. 2018; 100:56-
17 70. <https://doi.org/10.1016/j.bios.2017.08.058>.
18
19
20 28. Zhang J, Li B, Yue H, Wang J, Zheng Y. Highly selective and efficient imprinted polymers
21 based on carboxyl-functionalized magnetic nanoparticles for the extraction of gallic acid from
22 pomegranate rind. *J Separation Sci*. 2018; 41(2):540-547.
23
24 <https://doi.org/10.1002/jssc.201700822>.
25
26
27 29. Zhang M, Zhang X, He X, Chen L, Zhang Y. A self-assembled polydopamine film on the
28 surface of magnetic nanoparticles for specific capture of protein. *Nanoscale*. 2012; 4(10):
29 3141-3147. <https://doi.org/10.1039/c2nr30316g>.
30
31
32 30. Hu X, Xie L, Guo J, Li H, Jiang X, Zhang Y, Shi S. Hydrophilic gallic acid-imprinted
33 polymers over magnetic mesoporous silica microspheres with excellent molecular recognition
34 ability in aqueous fruit juices. *Food Chem*. 2015; 179:206-212.
35
36 <https://doi.org/10.1016/j.foodchem.2015.02.007>.
37
38
39 31. Zhang YZ, Zhang JW, Wang CZ, Zhou LD, Zhang QH, Yuan CS. Polydopamine-Coated
40 Magnetic Molecularly Imprinted Polymers with Fragment Template for Identification of
41 Pulsatilla Saponin Metabolites in Rat Feces with UPLC-Q-TOF-MS. *J Agric Food Chem*.
42 2018; 66(3):653-660. <https://doi.org/10.1021/acs.jafc.7b05747>.
43
44
45 32. Lv P, Xie D, Zhang Z. Magnetic carbon dots based molecularly imprinted polymers for
46 fluorescent detection of bovine hemoglobin. *Talanta*. 2018; 188:145-151.
47
48 <https://doi.org/10.1016/j.talanta.2018.05.068>.
49
50
51 33. Wang XN, Liang RP, Meng XY, Qiu JD. One-step synthesis of mussel-inspired molecularly
52 imprinted magnetic polymer as stationary phase for chip-based open tubular capillary
53 electrochromatography enantioseparation. *J Chromatogr A*. 2014; 1362:301-308.
54
55 <https://doi.org/10.1016/j.chroma.2014.08.044>.
56
57
58
59
60

- 1
2
3 34. Qiao L, Gan N, Hu F, Wang D, Lan H, Li T, Wang H. Magnetic nanospheres with a
4 molecularly imprinted shell for the preconcentration of diethylstilbestrol. *Microchim Acta*.
5 2014; 181(11-12):1341-1351. <https://doi.org/10.1007/s00604-014-1257-y>.
6
7
- 8 35. Jia X, Xu M, Wang Y, Ran D, Yang S, Zhang M. Polydopamine-based molecular imprinting
9 on silica-modified magnetic nanoparticles for recognition and separation of bovine
10 hemoglobin. *Analyst*. 2013; 138(2):651-658. <https://doi.org/10.1039/c2an36313e>.
11
12
- 13 36. Gao R, Zhang L, Hao Y, Cui X, Liu D, Zhang M, Tang Y. Novel polydopamine imprinting
14 layers coated magnetic carbon nanotubes for specific separation of lysozyme from egg white.
15 *Talanta*. 2015; 144:1125-1132. <https://doi.org/10.1016/j.talanta.2015.07.090>.
16
17
- 18 37. Wu W, Yang L, Zhao F, Zeng B. A vanillin electrochemical sensor based on molecularly
19 imprinted poly (1-vinyl-3-octylimidazole hexafluoride phosphorus)-multi-walled carbon
20 nanotubes@ polydopamine-carboxyl single-walled carbon nanotubes composite. *Sens.*
21 *Actuator B-Chem*. 2017; 239:481-487. <https://doi.org/10.1016/j.snb.2016.08.041>.
22
23
- 24 38. Yin ZZ, Cheng SW, Xu LB, Liu HY, Huang K, Li L, Zhai YY, Zeng YB, Liu HQ, Shao Y,
25 Zhang ZL, Lu YX. Highly sensitive and selective sensor for sunset yellow based on
26 molecularly imprinted polydopamine-coated multi-walled carbon nanotubes. *Biosens*
27 *Bioelectron*. 2018; 100:565-570. <https://doi.org/10.1016/j.bios.2017.10.010>
28
29
- 30 39. Yin Y, Yan L, Zhang Z, Wang J, Luo N. Polydopamine-coated magnetic molecularly
31 imprinted polymer for the selective solid-phase extraction of cinnamic acid, ferulic acid and
32 caffeic acid from radix scrophulariae sample. *Journal of separation science*. 2016; 39(8):1480-
33 1488. <https://doi.org/10.1002/jssc.201600026>.
34
35
- 36 40. Zhu X, Li H, Liu H, Peng W, Zhong S, Wang Y. Halloysite-based dopamine-imprinted
37 polymer for selective protein capture. *J Separation Sci*. 2016; 39(12):2431-2437.
38 <https://doi.org/10.1002/jssc.201600168>.
39
40
- 41 41. Chen F, Zhao W, Zhang J, Kong J. Magnetic two-dimensional molecularly imprinted
42 materials for the recognition and separation of proteins. *Phys Chem Chem Phys*. 2016;
43 18(2):718-725. <https://doi.org/10.1039/c5cp04218f>.
44
45
- 46 42. Luo J, Jiang S, Liu X. Efficient one-pot synthesis of mussel-inspired molecularly imprinted
47 polymer coated graphene for protein-specific recognition and fast separation. *J Phys Chem C*.
48 2013; 117(36):18448-18456. <https://doi.org/10.1021/jp405171w>.
49
50
- 51 43. Tretjakov A, Syritski V, Reut J, Boroznjak R, Volobujeva O, Öpik A. Surface molecularly
52 imprinted polydopamine films for recognition of immunoglobulin G. *Microchim Acta*. 2013;
53 180(15-16):1433-1442. <https://doi.org/10.1007/s00604-013-1039-y>.
54
55
56
57
58
59
60

- 1
2
3 44. Zhou WH, Tang SF, Yao QH, Chen FR, Yang HH, Wang XR. A quartz crystal microbalance
4 sensor based on mussel-inspired molecularly imprinted polymer. *Biosens Bioelectron.* 2010;
5 26(2):585-589. <https://doi.org/10.1016/j.bios.2010.07.024>.
6
7
8 45. Turco A, Corvaglia S, Mazzotta E, Pompa PP, Malitesta C. Preparation and characterization
9 of molecularly imprinted mussel inspired film as antifouling and selective layer for
10 electrochemical detection of sulfamethoxazole. *Sens Actuator B-Chem.* 2018; 255:3374-
11 3383. <https://doi.org/10.1016/j.snb.2017.09.164>.
12
13 46. Zhang YZ, Zhang JW, Wang CZ, Zhou LD, Zhang QH, Yuan CS. Polydopamine-Coated
14 Magnetic Molecularly Imprinted Polymers with Fragment Template for Identification of
15 Pulsatilla Saponin Metabolites in Rat Feces with UPLC-Q-TOF-MS. *J Agric Food Chem.*
16 2018; 66(3):653-660. <https://doi.org/10.1016/10.1021/acs.jafc.7b05747>.
17
18 47. Hashemi-Moghaddam H, Kazemi-Bagsangani S, Jamili M, Zavareh S. Evaluation of
19 magnetic nanoparticles coated by 5-fluorouracil imprinted polymer for controlled drug
20 delivery in mouse breast cancer model. *Int J Pharm.* 2016; 497(1-2):228-238.
21 <https://doi.org/10.1016/j.ijpharm.2015.11.040>.
22
23 48. Ouyang R, Lei J, Ju H. Surface molecularly imprinted nanowire for protein specific
24 recognition. *Chem Comm.* 2008; 44:5761-5763. <https://doi.org/10.1016/10.1039/b810248a>.
25
26 49. Gao R, Zhang L, Hao Y, Cui X, Tang Y. Specific removal of protein using protein imprinted
27 polydopamine shells on modified amino-functionalized magnetic nanoparticles. *RSC Adv.*
28 2014 ; 4(110):64514-64524. <https://doi.org/10.1039/c4ra07965e>.
29
30 50. Yang B, Gong H, Chen C, Chen X, Cai C. A virus resonance light scattering sensor based on
31 mussel-inspired molecularly imprinted polymers for high sensitive and high selective
32 detection of Hepatitis A Virus. *Biosens Bioelectron.* 2017; 87:679-685.
33 <https://doi.org/10.1016/j.bios.2016.08.087>.
34
35 51. Zhang F, Luo L, Gong H, Chen C, Cai C. A magnetic molecularly imprinted optical chemical
36 sensor for specific recognition of trace quantities of virus. *RSC Adv.* 2018; 8(56):32262-
37 32268. <https://doi.org/10.1039/c8ra06204h>.
38
39 52. Voccia D, Bettazzi F, Baydemir G, Palchetti I. Alkaline-Phosphatase-Based Nanostructure
40 Assemblies for Electrochemical Detection of microRNAs. *J Nanosci Nanotechnol.* 2015;
41 15(5):3378-3384. <https://doi:10.1166/jnn.2015.10201>.
42
43 53. Baydemir G, Bettazzi F, Palchetti I, Voccia D. Strategies for the development of an
44 electrochemical bioassay for tnf-Alpha detection by using a non-immunoglobulin bioreceptor.
45 *Talanta.* 2016; 141:141-147. <https://doi:10.1016/j.talanta.2016.01.021>.
46
47 54. Almeida LC, Correia JP, Viana AS. Electrochemical and optical characterization of thin
48
49
50
51
52
53
54
55
56
57
58
59
60

- polydopamine films on carbon surfaces for enzymatic sensors. *Electrochim Acta*. 2018; 263:480-489. <https://doi:10.1016/j.electacta.2018.01.077>.
55. Amiri M, Amali E, Nematollahzadeh A, Salehniya H. Poly-dopamine films: Voltammetric sensor for pH monitoring. *Sens Actuator B-Chem*. 2016; 228:53-58. <https://doi:10.1016/j.snb.2016.01.012>.
56. Ismail I, Okajima T, Kawauchi S, Ohsaka T. Studies on the early oxidation process of dopamine by electrochemical measurements and quantum chemical calculations. *Electrochim Acta*. 2016; 211:777-786. <https://doi:10.1016/j.electacta.2016.05.056>.
57. Ball V, Del Frari D, Toniazzi V, Ruch D. Kinetics of polydopamine film deposition as a function of pH and dopamine concentration: Insights in the polydopamine deposition mechanism. *J Colloid Interface Sci*. 2012; 386(1):366-372. <https://doi:10.1016/j.jcis.2012.07.030>.
58. Lee H, Rho J, Messersmith PB. Facile conjugation of biomolecules onto surfaces via mussel adhesive protein inspired coatings. *Adv Mater*. 2009; 21(4):431-434. <https://doi:10.1002/adma.200801222>.
59. Dai M, Huang T, Chao L, Xie Q, Tan Y, Chen C, Meng W. Horseradish peroxidase-catalyzed polymerization of l-DOPA for mono-/bi-enzyme immobilization and amperometric biosensing of H₂O₂ and uric acid. *Talanta*. 2016; 149:117-123. <https://doi:10.1016/j.talanta.2015.11.047>.
60. Chen T, Xu Y, Wei S, Li A, Huang L, Liu J. A signal amplification system constructed by bi-enzymes and bi-nanospheres for sensitive detection of norepinephrine and miRNA. *Biosens Bioelectron*. 2019; 124-125:224-232. <https://doi:10.1016/j.bios.2018.10.030>.
61. Zhou Y, Yin H, Sui C, Wang Y, Ai S. Photoelectrochemical detection of 5-hydroxymethylcytosine in genomic DNA based on M. HhaI methyltransferase catalytic covalent bonding. *Chem Eng J*. 2018; 19(357):94-102. <https://doi:10.1016/j.cej.2018.09.138>.
62. Huang KJ, Wang L, Wang HB, Gan T, Wu YY, Li J, Liu YM. Electrochemical biosensor based on silver nanoparticles-polydopamine-graphene nanocomposite for sensitive determination of adenine and guanine. *Talanta*. 2013; 114:43-48. <https://doi:10.1016/j.talanta.2013.04.017>.
63. Liu P, Bai FQ, Lin DW., Peng HP, Hu Y, Zheng YJ, Chen W, Liu AL, Lin XH. One-pot green synthesis of mussel-inspired myoglobin-gold nanoparticles-polydopamine-graphene polymeric bionanocomposite for biosensor application. *J Electroanal Chem*. 2016; 764:104-109. <https://doi:10.1016/j.jelechem.2016.01.020>.
64. Zhu Y, Lu S, Manohari AG, Dong X, Chen F, Xu W, Shi Z, Xu C. Polydopamine

- interconnected graphene quantum dots and gold nanoparticles for enzymeless H₂O₂ detection. *J Electroanal Chem.* 2017; 796:75-81. <https://doi.org/10.1016/j.jelechem.2017.04.017>.
65. Loget G, Wood JB, Cho K, Halpern AR, Corn RM. Electrodeposition of polydopamine thin films for DNA patterning and microarrays. *Anal Chem.* 2013; 85(21):9991-9995. <https://doi:10.1021/ac4022743>.
66. Wan Y, Zhang D, Wang Y, Qi P, Hou B. Direct immobilisation of antibodies on a bioinspired architecture as a sensing platform. *Biosens Bioelectron.* 2011; 26(5):2595-2600. <https://doi:10.1016/j.bios.2010.11.013>.
67. Wang L, Miao L, Yang H., Yu J, Xie Y, Xu L, Song Y. A novel nanoenzyme based on Fe₃O₄ nanoparticles@thionine-imprinted polydopamine for electrochemical biosensing. *Sens Actuator B-Chem.* 2017; 253:108-114. <https://doi:10.1016/j.snb.2017.06.132>.
68. Cheng HY, Strobe E, Adams RN Electrochemical Studies of the Oxidation Pathways of Apomorphine. *Anal Chem.* 1979, 51(13):2243-2246. <https://doi:10.1021/ac50049a042>.
69. Łuczak T. Preparation and characterization of the dopamine film electrochemically deposited on a gold template and its applications for dopamine sensing in aqueous solution. *Electrochim Acta.* 2008; 53(19):5725–5731. <https://doi.org/10.1016/j.electacta.2008.03.052>.
70. Vatrál J, Boča R, Linert W. Oxidation properties of dopamine at and near physiological conditions. *Monatsh Chem.* 2015; 146(11):1799-1805. <https://doi:10.1007/s00706-015-1560-2>.
71. Kanyong P, Rawlinson S, Davis J. Fabrication and electrochemical characterization of polydopamine redox polymer modified screen-printed carbon electrode for the detection of guanine. *Sens Actuator B-Chem.* 2016; 233:528–534. <https://doi.org/10.1016/j.snb.2016.04.099>.
72. Zangmeister RA, Morris TA, Tarlov MJ. Characterization of polydopamine thin films deposited at short times by autoxidation of dopamine. *Langmuir.* 2013; 29(27):8619-8628. <https://doi:10.1021/la400587j>.
73. Voccia D, Sosnowska M, Bettazzi F, Roscigno G, Fratini E, De Franciscis V, Condorelli G, Chitta R, D'Souza F, Kutner W, Palchetti I. Direct determination of small RNAs using a biotinylated polythiophene impedimetric genosensor. *Biosens Bioelectron.* 2017; 87:1012-1019. <https://doi:10.1016/j.bios.2016.09.058>.
74. Bettazzi F, Voccia D, Bencini A, Giorgi C, Palchetti I, Valtancoli B, Conti L. Optical and Electrochemical Study of Acridine-Based Polyaza Ligands for Anion Sensing. *Eur J Inorg Chem.* 2018; 23:2675-2679. <https://doi:10.1002/ejic.201800298>.
75. Zhou Y, Yin H, Sui C, Wang Y, Ai S. Photoelectrochemical detection of 5-hydroxymethylcytosine in genomic DNA based on M. HhaI methyltransferase catalytic covalent bonding. *Chem Eng J* 2019; 357:94–102. <https://doi.org/10.1016/j.cej.2018.09.138>.
76. Yu Y, Huang Z, Zhou Y. Facile and highly sensitive photoelectrochemical biosensing

- platform based on hierarchical architected polydopamine/tungsten oxide nanocomposite film. *Biosens Bioelectron.* 2019; 126:1-6. <https://doi.org/10.1016/j.bios.2018.10.026>.
77. Bettazzi F, Laschi S, Voccia D, Gellini C, Pietraperzia G, Falciola L, Pifferi V, Testolin A, Ingrosso C, Placido T, Comparelli R, Curri ML, Palchetti I. Ascorbic acid-sensitized Au nanorods-functionalized nanostructured TiO₂ transparent electrodes for photoelectrochemical genosensing. *Electrochim Acta.* 2018; 276:389-398. <https://doi.org/10.1016/j.electacta.2018.04.146>.
78. Li J, Li X, Zhao Q, Jiang Z, Tadé M, Wang S, Liu S. Polydopamine-assisted decoration of TiO₂ nanotube arrays with enzyme to construct a novel photoelectrochemical sensing platform. *Sens Actuator B-Chem.* 2018; 255:133-139. <https://doi.org/10.1016/j.snb.2017.06.168>.
79. Bettazzi F, Palchetti I. Photoelectrochemical genosensors for the determination of nucleic acid cancer biomarkers. *Curr Opin Electrochem.* 2018; 1-9. <https://doi.org/10.1016/j.coelec.2018.07.001>.
80. Wang R, Ma H, Zhang Y, Wang Q, Yang Z, Du B, Wu D, Wei Q. Photoelectrochemical sensitive detection of insulin based on CdS/polydopamine co-sensitized WO₃ nanorod and signal amplification of carbon nanotubes@polydopamine. *Biosens Bioelectron.* 2017; 96:345–350. <https://doi.org/10.1016/j.bios.2017.05.029>.
81. Çakıroğlu B, Özacar M. A self-powered photoelectrochemical glucose biosensor based on supercapacitor Co₃O₄-CNT hybrid on TiO₂. *Biosens Bioelectron.* 2018; 119:34–41. <https://doi.org/10.1016/j.bios.2018.07.049>.
82. Son EJ, Kim JH, Kim K, Park CB Quinone and its derivatives for energy harvesting and storage materials. *J Mater Chem-A.* 2016; 4(29):11179–11202. <https://doi.org/10.1039/c6ta03123d>.
83. Nam HJ, Kim B, Ko MJ, Jin M, Kim JM, Jung DY. A new mussel-inspired polydopamine sensitizer for dye-sensitized solar cells: Controlled synthesis and charge transfer. *Chem Eur J.* 2012; 18(44):14000–14007. <https://doi.org/10.1002/chem.201202283>.
84. Feng J, Li F, Li X, Wang Y, Fan D, Du B, Li Y, Wei Q. Label-free photoelectrochemical immunosensor for NT-proBNP detection based on La-CdS/3D ZnIn₂S₄/Au@ZnO sensitization structure. *Biosens Bioelectron.* 2018; 117:773–780. <https://doi.org/10.1016/j.bios.2018.07.015>.
85. Karakouz T, Holder D, Goomanovsky M, Vaskevich A, Rubinstein I. Morphology and refractive index sensitivity of gold island films. *Chem Mater.* 2009; 21:5875-215885. <https://doi.org/10.1021/cm902676d>.

- 1
2
3 86. Tesler AB, Chuntunov L, Karakouz T, Bendikov TA, Haran G, Vaskevich A, Rubinstein I.
4 Tunable localized plasmon transducers prepared by thermal dewetting of percolated
5 evaporated gold films. J Phys Chem C. 2011; 115:24642-24652.
6 <https://doi:10.1021/jp209114j>.
7
8
9
10
11
12
13
14
15
16
17
18
19
20
21
22
23
24
25
26
27
28
29
30
31
32
33
34
35
36
37
38
39
40
41
42
43
44
45
46
47
48
49
50
51
52
53
54
55
56
57
58
59
60

For Peer Review

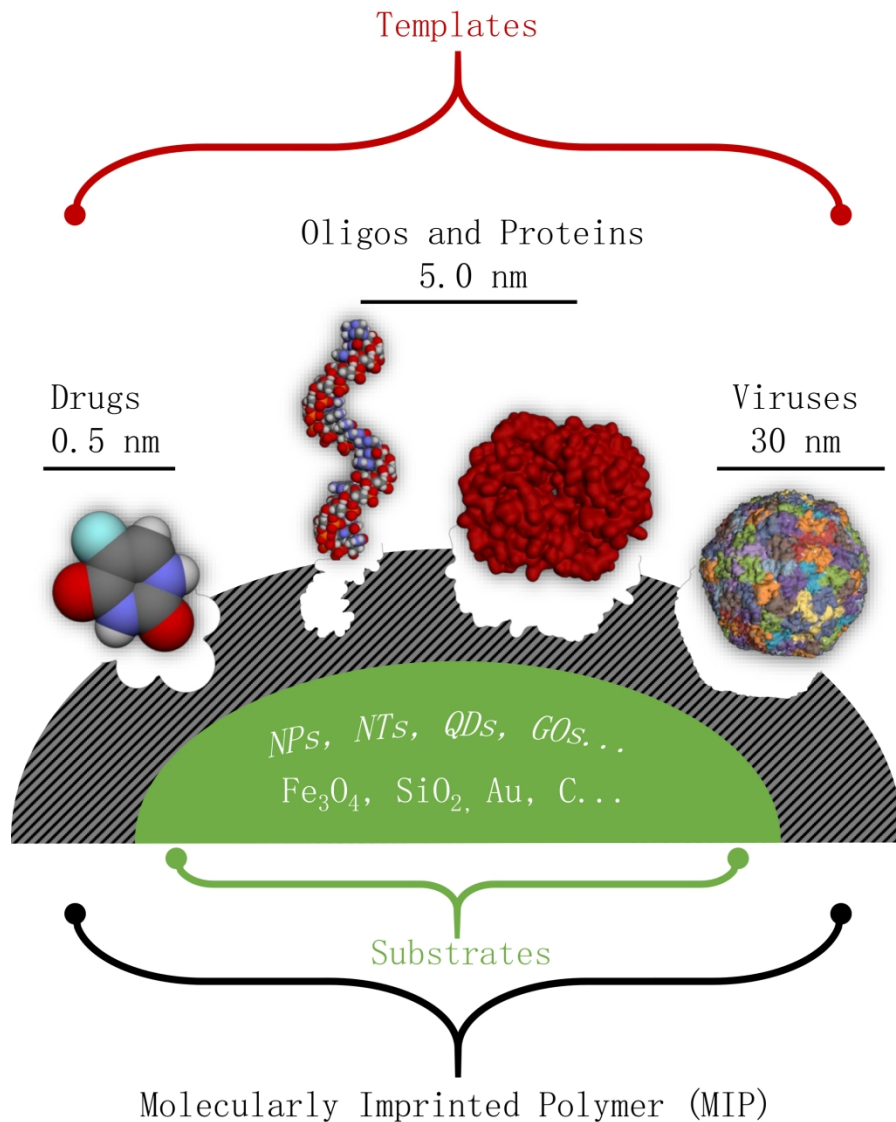
Figure legends

Fig. 1 Schematic representation of PDA imprinting on substrates with several kinds of geometries and composition. Dopamine-template co-polymerization and the subsequent template removal generates synthetic binding sites within the polymer with a broad range of dimension.

Fig. 2 (a-b) PDA electropolymerization by CV at screen-printed carbon electrode (5.0 mM DA, pH 7.0, 100 mV s⁻¹), reprinted with permission from [71]. (c) Mechanism of photo-induced charges separation caused by the PDA. Polydopamine-assisted decoration of TiO₂ nanotube arrays with HRP and subsequent photocurrent decrease in the presence of H₂O₂ due to insoluble enzymatic product formation. Redrawn with permission from [78].

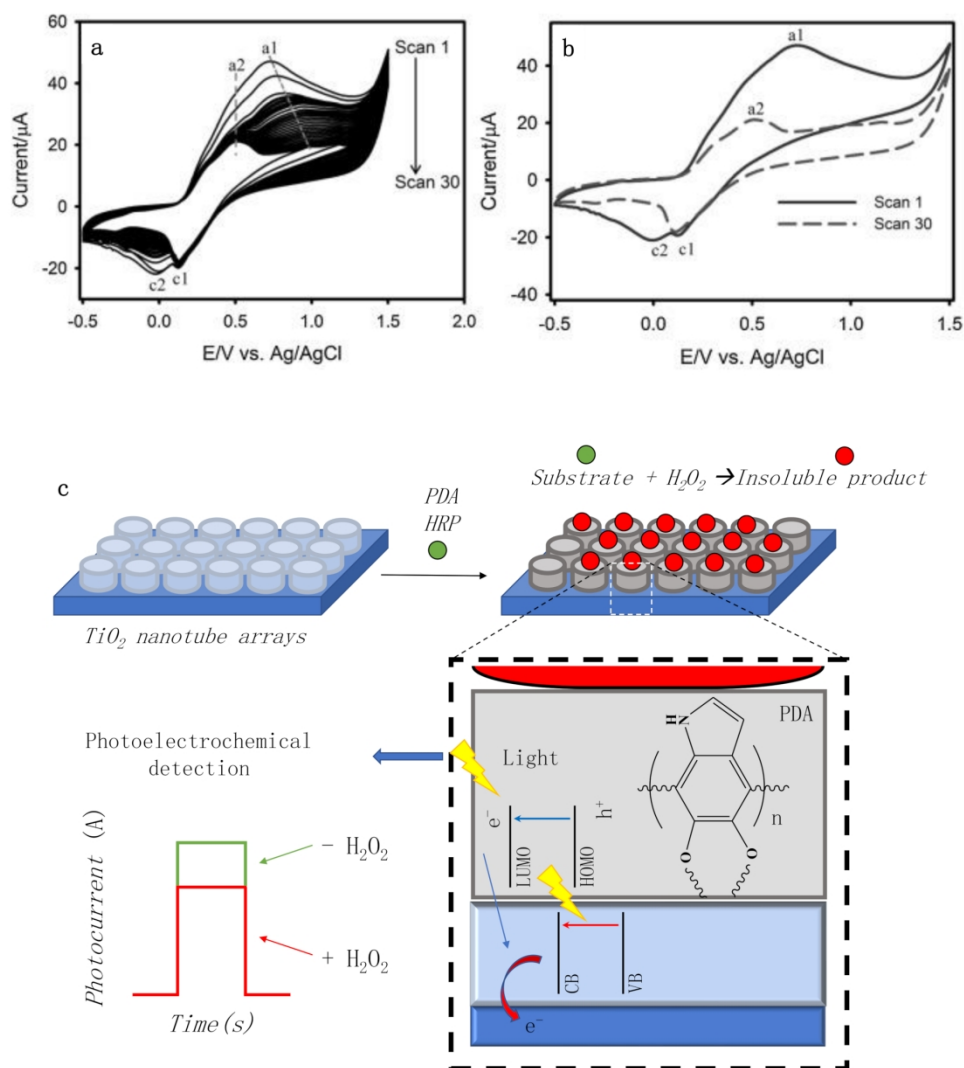
Fig. 3 Innovative uses of PDA in the field of (bio)analytical chemistry. (a) Competition-based assay for quantification of total protein in biological fluids. (b) (LSPR)-based quantitative assay at fixed wavelength for applications in clinical, food, and environmental controls. (c) Catalytic-based assay for redox reactions.

For Peer Review



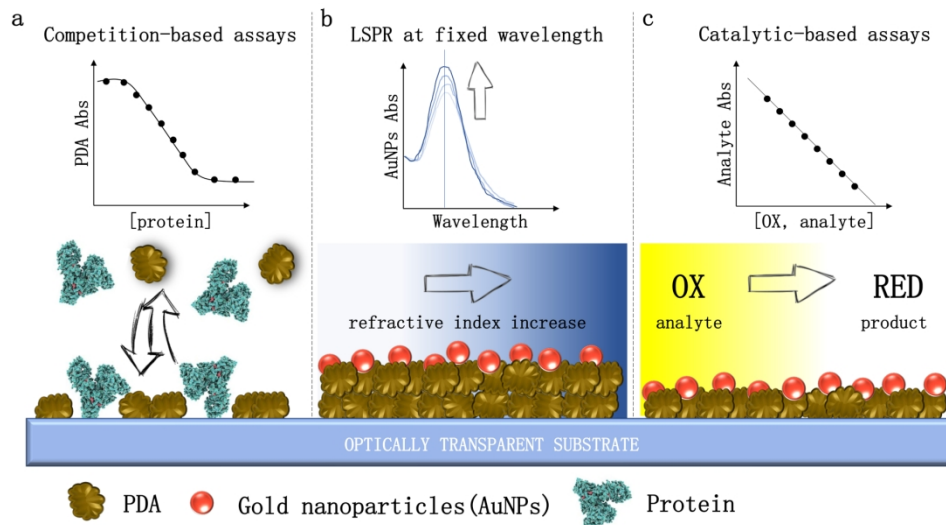
45 Schematic representation of PDA imprinting on substrates with several kinds of geometries and composition.
46 Dopamine-template co-polymerization and the subsequent template removal generates synthetic binding
47 sites within the polymer with a broad range of dimension.

48 173x233mm (300 x 300 DPI)
49
50
51
52
53
54
55
56
57
58
59
60



(a-b) PDA electropolymerization by CV at screen-printed carbon electrode (5.0 mM DA, pH 7.0, 100 mV s⁻¹), reprinted with permission from [71]. (c) Mechanism of photo-induced charges separation caused by the PDA. Polydopamine-assisted decoration of TiO₂ nanotube arrays with HRP and subsequent photocurrent decrease in the presence of H₂O₂ due to insoluble enzymatic product formation. Redrawn with permission from [78].

173x192mm (300 x 300 DPI)



Innovative uses of PDA in the field of (bio)analytical chemistry. (a) Competition-based assay for quantification of total protein in biological fluids. (b) (LSPR)-based quantitative assay at fixed wavelength for applications in clinical, food, and environmental controls. (c) Catalytic-based assay for redox reactions.

173x97mm (300 x 300 DPI)